

# Richardson's Barotropic Forecast: A Reappraisal

Peter Lynch  
Irish Meteorological Service,  
Glasnevin Hill, Dublin 9, Ireland

## Abstract

To elucidate his numerical technique and to examine the effectiveness of geostrophic initial winds, Lewis Fry Richardson carried out an idealized forecast using the linear shallow-water equations and simple analytical pressure and velocity fields. This barotropic forecast has been repeated and extended using a global numerical model, and the results are presented in this paper. Richardson's conclusions regarding the use of geostrophic winds as initial data are reconsidered.

An analysis of Richardson's data into normal modes shows that almost 85% of the energy is accounted for by a single eigenmode, the gravest symmetric rotational Hough mode, which travels westward with a period of about five days. This five-day wave has been detected in analyses of stratospheric data. It is striking that the fields chosen by Richardson on considerations of smoothness should so closely resemble a natural oscillation of the atmosphere.

The numerical model employed in this study uses an implicit differencing technique, which is stable for large time steps. The numerical instability that would have destroyed Richardson's barotropic forecast, had it been extended, is thereby circumvented. It is sometimes said that computational instability was the cause of the failure of Richardson's baroclinic forecast, for which he obtained a pressure tendency value two orders of magnitude too large. However, the initial tendency is independent of the time step (at least for the explicit scheme used by Richardson). In fact, the spurious tendency resulted from the presence of unrealistically large high-frequency gravity-wave components in the initial fields.

High-frequency oscillations are also found in the evolution starting from the idealized data in the barotropic forecast. They are shown to be due to the gravity-wave components of the initial data. These oscillations may be removed by a slight modification of the initial fields. This initialization is effected by means of a simple digital filtering technique, which is applicable not only to the linear equations used here but also to a general nonlinear system.

## 1. Introduction

*Before attending to the complexities of the actual atmosphere . . . it may be well to exhibit the working of a much simplified case. (Richardson 1922, p. 4)*

The numerical weather forecast carried out manually by Lewis Fry Richardson in the second decade of this century was a triumphant scientific achievement. The true significance of his work was clouded by his unrealistic results, in particular the "glaring error" in the pressure tendency, for which he calculated a change of 145 hPa in 6 h. In view of these results, his decision to publish the book *Weather Prediction by Numerical Process* (Richardson 1922; denoted LFR) was an act

of considerable courage, as there were few who could appreciate the great worth of his brilliantly innovative research.

To clarify the essential steps required to obtain a numerical solution of the equations of motion, Richardson included in his book (LFR, chap. 2) an introductory example in which he integrated a linearized system equivalent to the shallow-water equations. For this example he used an idealized initial pressure field defined by a simple analytical formula, and corresponding winds derived from the geostrophic relationship. In the following, this barotropic forecast will be reexamined, and repeated and extended using a global numerical model.

A superlative review of Richardson's book by Platzman (1967) appeared on the occasion of the publication of the Dover paperback edition in 1965. This extensive article is a wonderfully readable account of Richardson's work, enriched by fascinating historical detail. Platzman wrote that he found the illustrative example in chapter 2 "one of the most interesting parts of the book!" Richardson's step-by-step description of his calculations is clear and explicit and is a splendid introduction to the process of numerical weather prediction. In contrast, the remainder of the book is heavy going, containing so much extraneous material that the central ideas are often obscured.

## 2. Richardson's model and data

The equations solved by Richardson are obtained by vertical integration of the primitive equations linearized about an isothermal, motionless basic state. They may be written as follows:

$$\frac{\partial u}{\partial t} - fv + \frac{\partial}{\partial x} \left( \frac{p'}{p_0} \right) = 0 \quad (1)$$

$$\frac{\partial v}{\partial t} + fu + \frac{\partial}{\partial y} \left( \frac{p'}{p_0} \right) = 0 \quad (2)$$

$$\frac{\partial}{\partial t} \left( \frac{p'}{p_0} \right) + gH \nabla \cdot \mathbf{V} = 0 \quad (3)$$

The dependent variables are the horizontal wind  $\mathbf{V} = (u, v)$  and the surface pressure perturbation  $p'$ . The independent variables are the time  $t$ , latitude  $\phi$ , and longitude  $\lambda$  ( $dx = a \cos \phi d\lambda$  and  $dy = a d\phi$  are distances

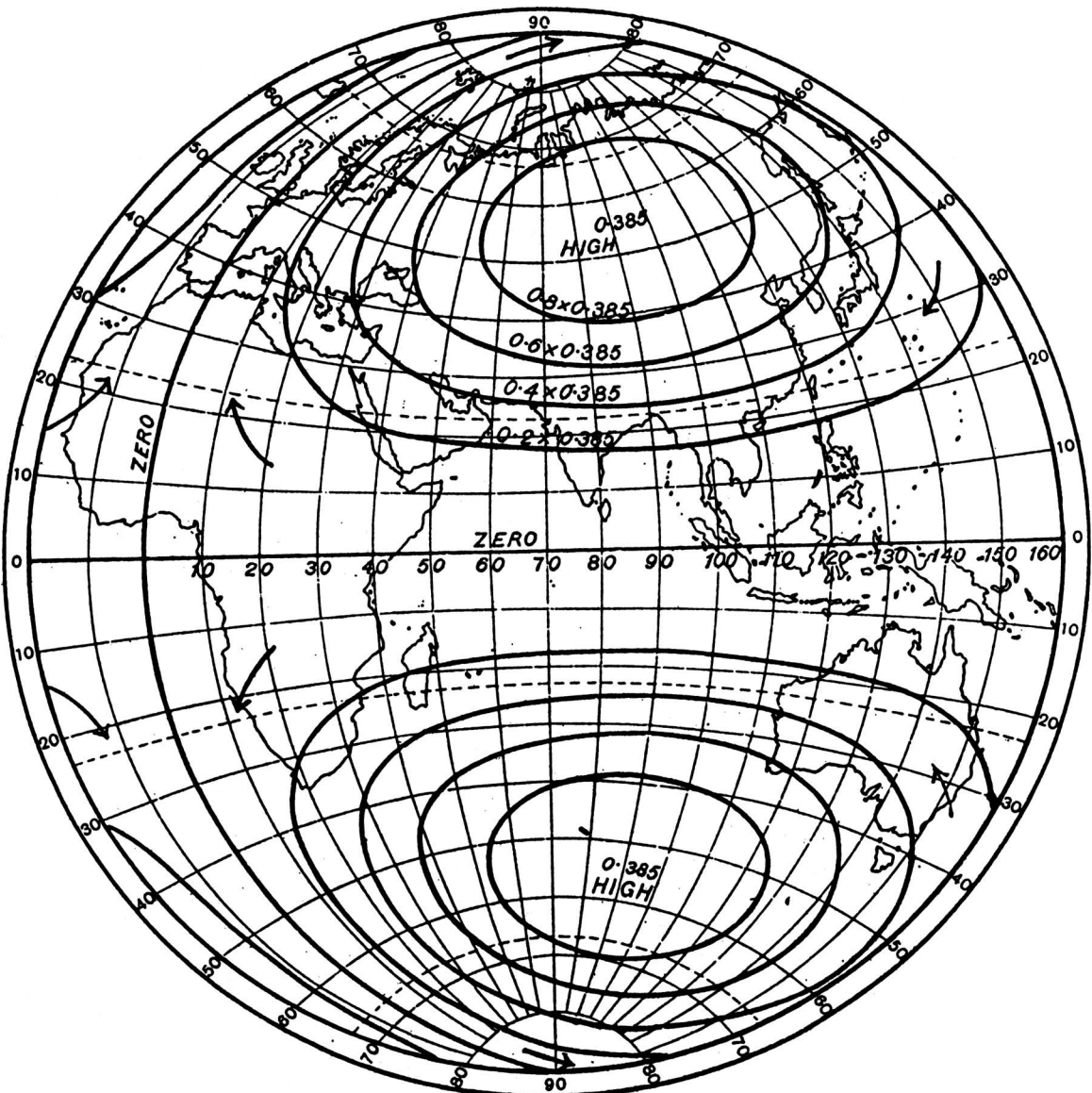


FIG. 1. The initial pressure field chosen by Richardson for his barotropic forecast (reproduced from LFR, p. 6).

eastward and northward on the globe). The earth's radius is  $2 \times 10^7 \pi^{-1} \text{ m} \doteq 6366 \text{ km}$ . The gravitational acceleration is  $g = 9.79 \text{ m s}^{-2}$ , and  $f = 2\Omega \sin\phi$  is the Coriolis parameter. The scale height  $H = RT_0 g^{-1}$  was set at 9.2 km, corresponding to a mean temperature  $T_0 = 314 \text{ K}$ , somewhat larger than one might expect. The value chosen for  $H$  was based on observations carried out by W. H. Dines (LFR, p. 4). The reference density  $\rho_0$  may be determined by fixing the mean surface pressure; taking  $p_0 = 1000 \text{ hPa}$ , it is approximately  $1.1 \text{ kg m}^{-3}$ . The familiar velocity form of the equations of motion has been used here, although Richardson wrote the equations in terms of vertically integrated momentum. He used the cgs system of units; the momentum values on page 8 of LFR are approxi-

mately equivalent to the SI values of wind speed multiplied by  $10^5$ ; his pressure values are numerically equal to pressure in microbars or deciPascals.

The Eqs. (1)–(3) are mathematically isomorphic to the linear shallow-water equations that govern the small-amplitude dynamics of an incompressible homogeneous shallow fluid layer on a sphere. In this case one interprets  $H$  as the mean depth and equates  $(p'/\rho_0)$  to  $\Phi' = gh'$ , the geopotential perturbation of the free surface. The equations are also called the Laplace Tidal Equations and their solutions have been studied extensively by both analytical and numerical means.

The initial pressure perturbation chosen by Richardson is depicted in Fig. 1. It is a simple zonal wavenumber-one perturbation, given by

$$p' = 10^4 \sin^2\phi \cos\phi \sin\lambda \text{ (Pa)}, \quad (4)$$

which is symmetric about the equator with maxima of magnitude 38.5 hPa at 90°E and 55°N and S, and corresponding minima in the western hemisphere at the antipodes of the maxima. The initial winds were taken to be in geostrophic balance with the pressure field, and are given by

$$u = -(10^4/2\Omega a \rho_0)(2\cos^2\phi - \sin^2\phi) \sin\lambda \text{ (m s}^{-1}) \quad (5)$$

$$v = (10^4/2\Omega a \rho_0) \sin\phi \cos\lambda \text{ (m s}^{-1}). \quad (6)$$

The maximum velocity is about 20 m s<sup>-1</sup> zonally along the equator.

Figure 1 is an “elevation” view of the eastern hemisphere on what appears to be a globular or equidistant projection. This is reproduced from page 6 of Richardson’s book and is also featured on the cover of the Dover edition. It is surprising that the Antarctic coastline, well known long before Richardson’s day, is unmarked on the background map.<sup>1</sup> A “plan” view of the initial fields in the northern hemisphere, on a polar stereographic projection, is shown in Fig. 4(a).

### 3. The barotropic forecast

Richardson calculated the initial changes in pressure and wind (or momentum) using a finite difference method. He selected a time step of 2700 s, or 3/4 h, and used a spatial grid analogous to a chessboard, with pressure evaluated at the center of the black squares and winds at the center of the white. The frontispiece of LFR shows such a grid, displaced 2° west from that used in his introductory example. Today such a discretization is called an E-grid, following the classification introduced by Arakawa; however, the appellation “Richardson Grid,” proposed by Platzman, would perhaps be better. The distance between adjacent squares of like color is 400 km in latitude, with 64 such squares around each parallel. This implies grid intervals of  $\Delta\lambda = 5.625^\circ$ ,  $\Delta\phi = 3.6^\circ$ . The resolution at 50°N is about the same in both directions. The advantage of the chessboard pattern is that the time rates are given at the points where the variables are initially tabulated. Thus, the integration process can be con-

tinued without limit and is in Richardson’s words “lattice reproducing.” The chessboard pattern is depicted in Fig. 2 (from Platzman 1967).

The changes in pressure and momentum were calculated for a selection of points near England and entered in the table on page 8 of LFR. The focus here will be on the pressure tendency at the grid point 5600 km north of the equator and on the prime meridian (the coordinates are 50.4°N, 0°E, and the point lies in the center of the English Channel, south of Sussex). The value obtained by Richardson was a change of 2.621 hPa in 3/4 h. This rise suggests a westward movement of the pressure pattern (similar rises were found at adjacent points). Such a movement is confirmed by use of the geostrophic wind relation in the pressure-tendency equation (3). The divergence corresponding to geostrophic flow is

$$\nabla \cdot V_g = (-\beta/f) v_g = (-\beta/\rho_0 f^2) \frac{\partial p'}{\partial x},$$

where the “beta parameter” is  $\beta = \partial f/\partial y$ . This implies convergence for poleward flow and divergence for equatorward flow. Since the initial winds are geostrophic, the initial tendency determined from (3) is

$$\frac{\partial p'}{\partial x} = (g H \beta / f^2) \frac{\partial p'}{\partial x} \quad (7)$$

[LFR, Eq. (8)]. This means that “where pressure increases towards the east, there the pressure is rising if the wind be momentarily geostrophic” (LFR, p. 9). Richardson argues that this deduction indicates that the geostrophic wind is inadequate for the computation of pressure changes.

The right-hand side of (7) is easily calculated for the chosen pressure perturbation (4). The parameter values are  $a = 2 \times 10^7 \pi^{-1}$  m,  $g = 9.79$  m s<sup>-2</sup>,  $H = 9.2$  km,  $2\Omega = 1.458 \times 10^{-4}$  s<sup>-1</sup>, in agreement with LFR, page 13. At the point in question, the tendency calculated from (7) comes to 0.09713 Pa s<sup>-1</sup> or 2.623 hPa in 3/4 h. This analytical value is very close to the numerical value (2.621) calculated by Richardson, indicating that errors due to spatial discretization are small. The assumption of geostrophy implies zero initial tendencies for the velocity components; this follows immediately from (1) and (2). The calculated initial changes of momentum obtained by Richardson were indeed very small, confirming the accuracy of his numerical technique.

Richardson, pointing out that “actual cyclones move eastward,” described a result of observational analysis that showed a negative correlation between  $\partial p'/\partial t$  and  $\partial p'/\partial x$ , in direct conflict with (7). In fact, the generally eastward movement of pressure disturbances in middle latitudes is linked to the strong

<sup>1</sup>There is another curiosity about the background map in Fig. 1: The island marked near 50°S, 80°E is 10° east of its correct position. This island was discovered by Kerguelen in 1772 but his determination of its longitude was inaccurate. The following year, James Cook, on his second voyage, crossed the assigned latitude 10° too far east and failed to find it (Debenham 1929). It is interesting that the position of the island marked in Fig. 1 coincides with Kerguelen’s original estimated location.

prevailing westerly flow in the upper troposphere. Presumably, Richardson was unaware of the dominant influence of the jet stream, whose importance became evident only with the development of commercial aviation.

Richardson was free to choose independent initial fields of pressure and wind, but “it has been thought to be more interesting to sacrifice the arbitrariness in order to test our familiar idea, the geostrophic wind, by assuming it initially and watching the ensuing changes” (LFR, p. 5). Recall that he worked out the introductory example in 1919, perhaps at W. H. Dines’ suggestion (the chapter ends with an acknowledgment to Dines; LFR, p. 15). He had ascribed the failure of his baroclinic forecast to erroneous initial winds. He wanted to examine the efficacy of geostrophic winds and, moreover, Eq. (7), which follows from the geostrophic assumption, allowed him to compare the results of his numerical process with the analytical solution for the initial tendency. As has been seen above, the numerical errors were negligible. However, the implication of (7) for the westward movement of pressure disturbances led him to infer that the geostrophic wind is inadequate for the calculation of pressure changes. Toward the end of the chapter, he concludes: “It has been made abundantly clear that a geostrophic wind behaving in accordance with the linear equations (1), (2), (3) cannot serve as an illustration of a cyclone.” He then questions whether the inadequacy resides in the equations or in the initial geostrophic wind, or in both, and suggests that further analysis of weather maps is indicated.

Was Richardson’s conclusion on the inappropriateness of geostrophic initial conditions justified? It is clear from a historical perspective that the reason that his simple forecast lacked verisimilitude lies elsewhere. The zonal component of the geostrophic relationship is obtained by omitting the time derivative in (2). Taking the vertical derivative of this (allowing for variations of density) and using the hydrostatic equation and the logarithmic derivative of the equation of state, one obtains the thermal wind equation:

$$\frac{\partial u_g}{\partial z} = - \left( \frac{g}{fT} \right) \frac{\partial T}{\partial y} + \left( \frac{u_g}{T} \right) \frac{\partial T}{\partial z}. \quad (8)$$

The second term on the right may be neglected by comparison with the first. Taking a modest value of 30 K for the pole-to-equator surface temperature difference, and assuming that this is representative of the meridional temperature gradient in the troposphere, (8) implies a westerly shear of about  $10 \text{ m s}^{-1}$  between the surface and the tropopause. Thus, if the winds near the surface are light, there must be a marked westerly flow aloft. Although the importance of the jet

stream was unknown in Richardson’s day, the above line of reasoning was obviously available to him. Yet, he focused on the geostrophic wind as the cause of lack of agreement between his forecast and the observed behavior of cyclones in middle latitudes. Surely, the real reason for this was his assumption of a barotropic structure for his disturbance, in contrast to the profoundly baroclinic nature of extratropical depressions.

Richardson might have incorporated the bulk effect of the jet stream on his perturbation by linearizing the equations about a westerly flow. Platzman has opined that Richardson’s “disregard of perturbation theory as a means of clarifying the problems of dynamic meteorology” was a major defect in his approach to weather prediction (Platzman 1967, p. 530).

#### 4. The global numerical model

Richardson’s forecast has been repeated and extended using a global barotropic numerical model based on the Laplace tidal equations (1), (2), and (3), the same linear equations as used by him. The same initial data were used and the same time step and spatial grid interval employed. There were only two substantive differences from Richardson’s method. First, an implicit timestepping scheme was used to insure numerical stability, in contrast to the explicit scheme of LFR, which is restricted by the Courant–Friedrichs–Lewy (CFL) criterion. Second, a C-grid was used for the horizontal discretization. The C-grid has zonal wind represented half a grid step east, and meridional wind half a grid step north of the pressure points. This grid was chosen when the model was first designed, for reasons that are irrelevant in the current context. Richardson’s grid comprises two C-grids superimposed, and coupled only through the Coriolis terms (Fig. 2). The initial pressure tendency calculated on one C-grid is independent of the other. The distribution of variables on the C-grid in the vicinity of the North Pole is shown in Fig. 3 (from McDonald and Bates 1989).

The CFL criterion requires that the time step of an explicit scheme be chosen to satisfy an inequality of the form

$$Le \equiv \frac{c\Delta t}{\Delta x} \leq 1,$$

where  $c$  is the maximum wave speed. This nondimensional parameter is often called the Courant number, but is denoted here as  $Le$  for Lewy, who discovered the stability criterion (Reid 1976, p. 116). The advantage of implicit differencing is that the CFL

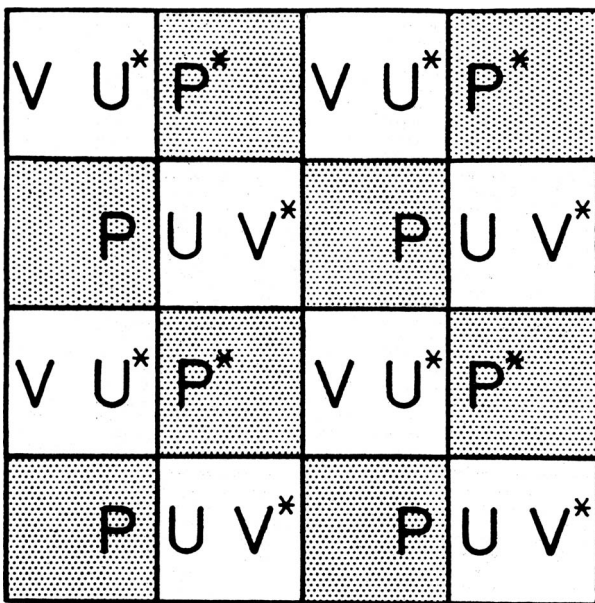


FIG. 2. The Richardson grid. Pressure is evaluated at the center of the black squares and winds at the center of white. The grid is comprised of two C-grids, one composed of the quantities marked by asterisks, the other composed of the remaining quantities. (From Platzman 1967.)

condition no longer applies and a longer time step may be used.

The numerical scheme used is a linear version of the two-time-level scheme devised by McDonald (1986). The momentum equations (1) and (2) are integrated in two half-steps,  $\Delta t/2$ . In the first half-step, the Coriolis terms are treated implicitly and the pressure-gradient terms explicitly:

$$(u^{n+\frac{1}{2}} - u^n) - Fv^{n+\frac{1}{2}} + D\Phi_x^n = 0 \quad (9)$$

$$(v^{n+\frac{1}{2}} - v^n) + Fu^{n+\frac{1}{2}} + D\Phi_y^n = 0. \quad (10)$$

Here  $\Phi = p'/\rho_0$ ,  $D = \Delta t/2$ , and  $F = f\Delta t/2$ . In the second half-step, the Coriolis terms are explicit, while the pressure-gradient terms are implicit:

$$(u^{n+1} - u^{n+\frac{1}{2}}) - Fv^{n+\frac{1}{2}} + D\Phi_x^{n+1} = 0 \quad (11)$$

$$(v^{n+1} - v^{n+\frac{1}{2}}) + Fu^{n+\frac{1}{2}} + D\Phi_y^{n+1} = 0. \quad (12)$$

If (9) and (10) are solved for  $u^{n+1/2}$  and  $v^{n+1/2}$ , these quantities can be eliminated from (11) and (12), yielding:

$$u^{n+1} + D\Phi_x^{n+1} = R_u \quad (13)$$

$$v^{n+1} + D\Phi_y^{n+1} = R_v. \quad (14)$$

The right-hand terms  $\mathbf{R} = (R_u, R_v)$  depend on the

variables at time  $n\Delta t$ . An expression for the divergence at time  $(n+1)\Delta t$  follows from these equations:

$$\nabla \cdot \mathbf{V}^{n+1} + D\nabla^2 \Phi^{n+1} = \nabla \cdot \mathbf{R}. \quad (15)$$

The continuity equation (3) is integrated in a single step  $\Delta t$ :

$$(\Phi^{n+1} - \Phi^n) + \bar{\Phi}D(\nabla \cdot \mathbf{V}^{n+1} + \nabla \cdot \mathbf{V}^n) \quad (16)$$

where  $\bar{\Phi} = gH$ . Elimination of the divergence between (15) and (16) yields an equation for  $\Phi^{n+1}$ :

$$[\nabla^2 - K^2] \Phi^{n+1} = R_\Phi, \quad (17)$$

where  $K^2 = 1/(\bar{\Phi}^2 D^2)$ , and the right-hand forcing is calculated from variables at  $n\Delta t$ . This Helmholtz equation is solved by the method of Sweet (1977). With  $\Phi^{n+1}$  known,  $u^{n+1}$  and  $v^{n+1}$  follow from (13) and (14). The simple form of (17) is a consequence of splitting the integration of the momentum equations into two half-steps. However, the splitting is formal, and no  $(n+1/2)$ -level quantities are actually computed. An analysis of the scheme is undertaken in McDonald (1986) and it is shown to be unconditionally stable and to have a time truncation of  $O(\Delta t^2)$ .

## 5. Extending the forecast

The pressure and wind selected by Richardson and specified by (4), (5), and (6) are shown in Fig. 4a.

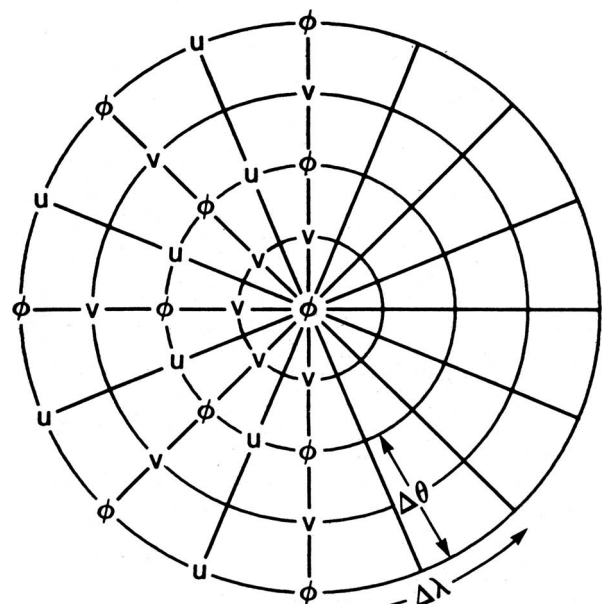


FIG. 3. The distribution of variables on the C-grid in the vicinity of the North Pole.

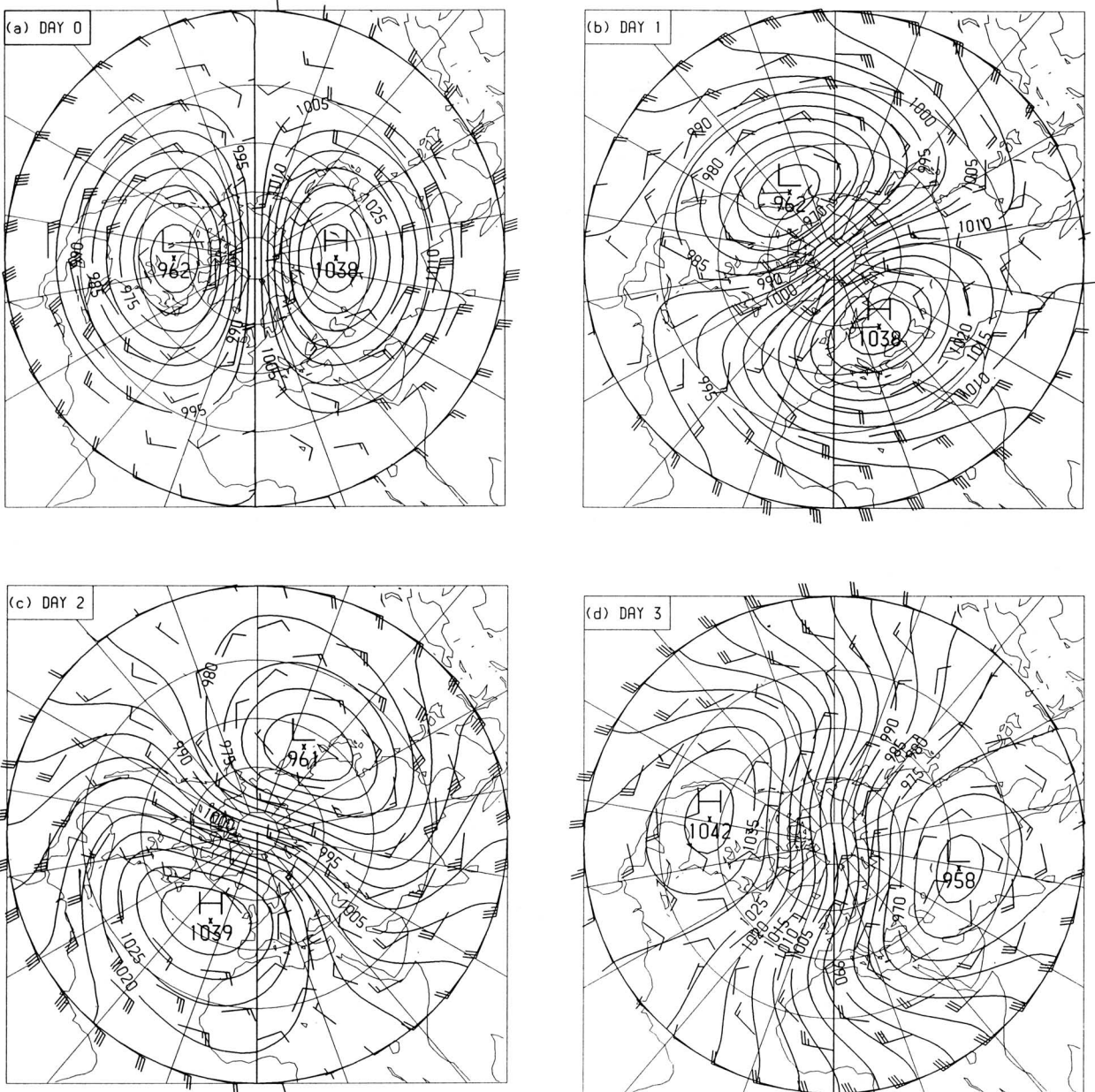


FIG. 4. (a) The initial fields of pressure and winds in the Northern Hemisphere. (b)–(f) Forecasts valid every 24 h from one to five days; (e) and (f) on next page.

Figures 4b–f show the forecast fields valid every 24 h, out to five days. Only the Northern Hemisphere is plotted, as the fields south of the equator are a mirror image of those shown. The initial change in pressure at the location  $50.4^{\circ}\text{N}$ ,  $0^{\circ}\text{E}$  was 2.601 hPa in 3/4 h. This is close to Richardson's value (2.621), the slight difference being due to the implicit timestepping scheme. The wavenumber-one perturbation rotates westward, almost circumnavigating the globe in five days. The pattern is substantially unchanged in extratropical regions. In the tropics, a zonal pressure gradient, absent in the initial field, develops and is maintained thereafter.

One may ask why the chosen perturbation is so robust, sustaining a coherent structure for such a long time and undergoing little change save for the retrogressive or westward rotation. This behavior is in fact attributable to the close resemblance of Richardson's chosen data to an eigensolution of his linear equations. These equations were first employed by Laplace to examine forced tidal motions. Their free or normal-mode solutions were studied by Hough and Margules, who found solutions falling into two categories. The first category comprised rapidly traveling progressive and retrogressive waves with large divergence fields; these are the gravity-inertia waves. The "oscillations

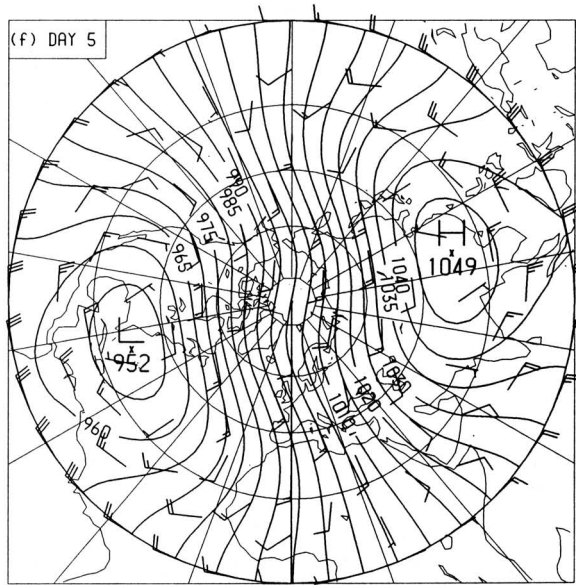
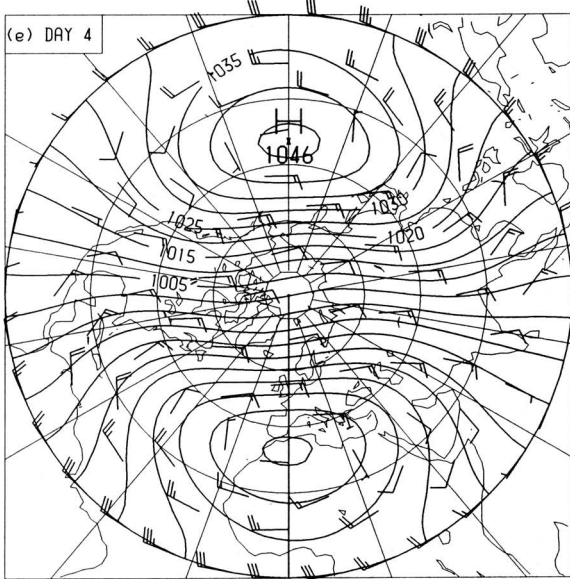


FIG. 4. (e) and (f), continued from previous page.

of the second class" were of lower frequency, with vorticity dominating divergence, and depending for their existence on the earth's rotation; they are referred to as rotational modes.

The dynamics of the second class of motions were greatly elucidated by Rossby and Haurwitz. Rossby (1939) assumed conservation of absolute vorticity on a beta plane and derived his now-famous formula for the wave speed:

$$c = \bar{u} - \frac{\beta L^2}{4\pi^2},$$

where  $\bar{u}$  is the zonal mean velocity,  $\beta$  the mean meridional variation of the Coriolis parameter, and  $L$  the wavelength. Haurwitz (1940) found the corresponding dispersion relation valid in spherical geometry:

$$c = \bar{u} - \frac{\beta a^2}{n(n+1)},$$

where  $n$  is the total wavenumber (the degree of the spherical harmonic solution), and showed that it corresponds to Margules' oscillations of the second class in the limit of nondivergent flow. The Rossby–Haurwitz waves are prototypical of the large-scale free waves in the atmosphere.

## 6. Hough function analysis

A more complete analysis of the solutions of the Laplace tidal equations has been undertaken by Longuet-Higgins (1968), Kasahara (1976), and others. The eigenfunctions of these equations are now called Hough functions. Figure 5 shows the meridional structure of height and wind for the first symmetric normal mode in each of the three categories, for zonal wavenumber one: Fig. 5a is the gravest, or largest-scale, rotational mode, Fig. 5b is the first eastward-traveling gravity wave, and Fig. 5c is the largest-scale westward-traveling gravity wave. These structures were calculated using the Fortran program in appendix B of Kasahara (1976). He used an equivalent depth of 10 km, not too far removed from Richardson's 9.2 km. Plots of several higher modes, and for other zonal wavenumbers, may be found in his paper. The solutions shown in Fig. 5 closely resemble the corresponding graphs in Figs. 4 and 5 of Kasahara (1976). The eigenfrequencies and periods of the lowest six symmetric modes in each of the three groups are given in Table 1 (these are for Richardson's value of  $H$ , and differ slightly from Kasahara's values). The largest symmetric rotational normal mode (Fig. 5a) has a period of about five days. This "five-day wave" has been unequivocally detected in the atmosphere (e.g., see Madden 1979). The primary eastward-traveling gravity wave (Fig. 5b) is known as the Kelvin wave.

The horizontal structure of the five-day wave is shown in Fig. 6a (with maximum amplitude of 38.5 hPa as for Richardson's field). The global model was integrated for five days using this wave as initial data, and the result is shown in Fig. 6b. It is practically indistinguishable from the initial field except for the angular displacement (it has almost completed a full revolution of the globe), consistent with the expected behavior of an eigenfunction. The initial pressure

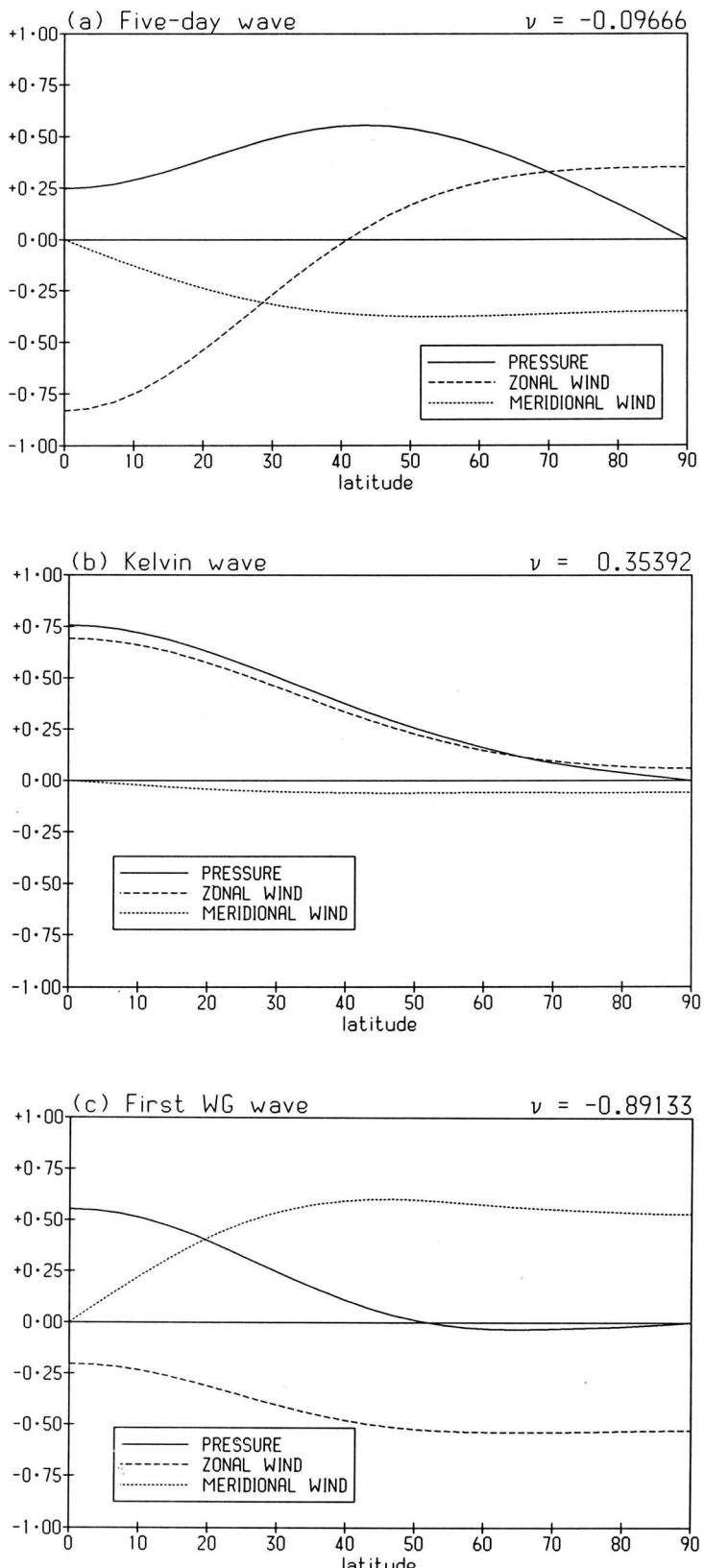


FIG. 5. Meridional structures of the primary symmetric rotational and gravity waves for zonal wavenumber one. (a) Rotational “five-day” wave. (b) Kelvin wave. (c) First westward-traveling gravity wave. The meridional velocity is  $90^\circ$  out of phase with the pressure and zonal wind.

tendency calculated for the five-day wave at the grid point at  $50.4^\circ\text{N}$ ,  $0^\circ\text{E}$  was 1.39 hPa in  $3/4$  h. Recall that Richardson's data produced an initial change of 2.62 hPa. Why the difference? Suppose that the pressure pattern (4) defined by Richardson were to rotate westward without change of form, making one circuit of the earth in a period  $\tau=5$  days. It could then be described by the equation

$$p'(t) = 10^4 \sin^2\phi \cos\phi \sin(\lambda + 2\pi t/\tau)$$

and the rate of change is obviously

$$\frac{\partial p'}{\partial t} =$$

$$\left(\frac{2\pi}{\tau}\right) 10^4 \sin^2\phi \cos\phi \cos(\lambda + 2\pi t/\tau),$$

which, at the point  $50.4^\circ\text{N}$ ,  $0^\circ\text{E}$  at time  $t=0$ , gives the value 1.44 hPa in  $3/4$  h, about half the value obtained by Richardson. One must conclude that the evolution of his pressure field involves more than a simple westward rotation with period  $\tau$ .

The meridional structures of Richardson's initial pressure and wind perturbations are shown in Fig. 7 (solid lines). Also shown are the structures of the five-day wave (dotted) and the Kelvin wave (dashed). A linear combination of these two modes, with respective weights of about 1.2 and -0.4, whose pressure vanishes at the equator, is also shown (dot-dash line). There is a close similarity between Richardson's data and the five-day wave in middle and high latitudes. Conversely, their structures in the tropics are quite different. The pressure structure of the combination of five-day and Kelvin waves is close to Richardson's curve everywhere; the wind fields are in fair agreement in this case. Thus, if Richardson's data is analyzed into a combination of Hough functions, one finds that the primary contribution is from the five-day wave, with the Kelvin wave second in importance, and less significant contributions from other normal modes.

To support the above qualitative argument, a more precise analysis of Richardson's data into Hough modes was performed, and the results are presented in Table 2. They show that almost 85% of the energy projects onto the five-day wave and about 11% resides in the Kelvin wave.

TABLE 1. Frequencies (nondimensional) and periods (in hours for gravity waves and days for rotational modes) of the lowest six symmetric modes in each of the three categories: eastward gravity waves, westward gravity waves, and Rossby-Haurwitz waves.

SYMMETRIC MODE NUMBER	EASTWARD GRAVITY WAVE	WESTWARD GRAVITY WAVE	ROSSBY-HAURWITZ WAVE
1	0.354 (33.9 h)	-0.891 (13.5 h)	-0.09666 (5.2 day)
2	1.241 (9.7 h)	-1.362 (8.8 h)	-0.03994 (12.5 day)
3	1.885 (6.4 h)	-1.925 (6.2 h)	-0.02131 (23.5 day)
4	2.515 (4.8 h)	-2.534 (4.7 h)	-0.01301 (38.4 day)
5	3.148 (3.8 h)	-3.160 (3.8 h)	-0.00871 (57.4 day)
6	3.786 (3.2 h)	-3.794 (3.2 h)	-0.00622 (80.4 day)

Over 99% of the energy is accounted for by only three of the Hough function components.

The time evolution of pressure at the chosen grid point, throughout the five-day period of the forecast starting from Richardson's data, is shown in Fig. 8. Also shown are the corresponding curves for zonal and meridional wind components (consider only the solid curves; the dashed curves will be discussed presently). The predominant variation of pressure is a single oscillation during the forecast, as one expects if the major component of the data is the five-day wave. There is a variation with a period of about 4/3 days and

smaller amplitude superimposed on this. Consulting Table 1, one sees that the period of the Kelvin wave is about 34 h, in agreement with this secondary variation. Note that the meridional wind is very small for this wave (see Fig. 5b). The two components are also found in the curve of zonal wind (Fig. 8, center panel), but the picture is complicated by the presence of further components. The situation is clarified by considering the variation of the meridional wind, the bottom panel of Fig. 8, since  $v$  is very small for the Kelvin wave. This curve shows a short-period oscillation, with about nine cycles in the five days, superim-

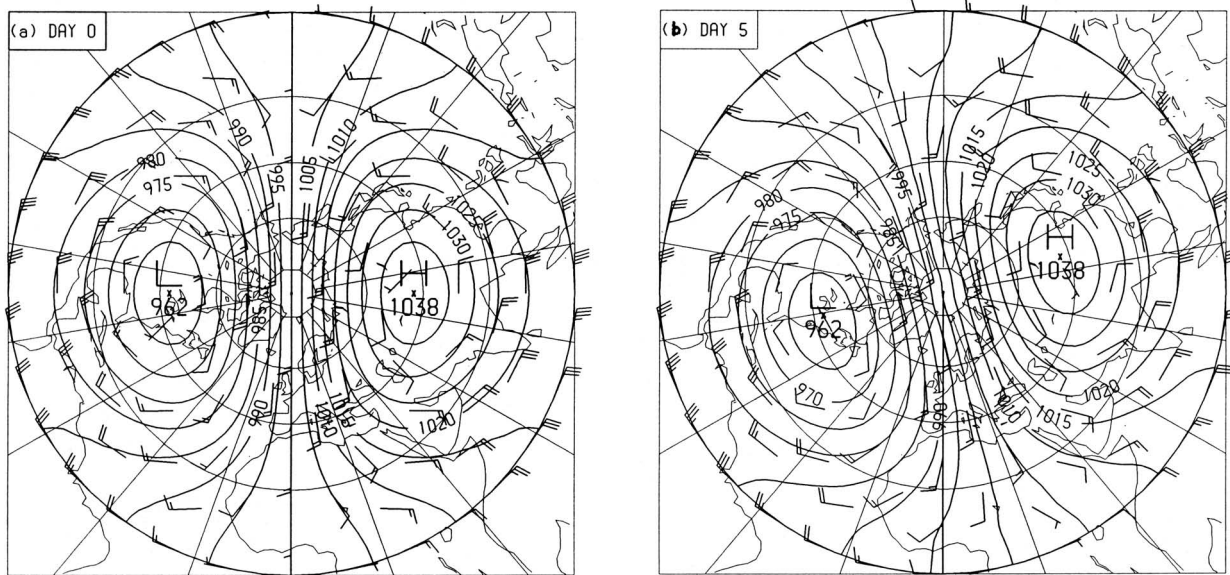


FIG. 6. The "five-day wave," the gravest symmetric rotational eigenfunction. (a) is chosen as the initial state, and (b) shows the forecast after five days, when the wave has almost completed a circuit of the globe.

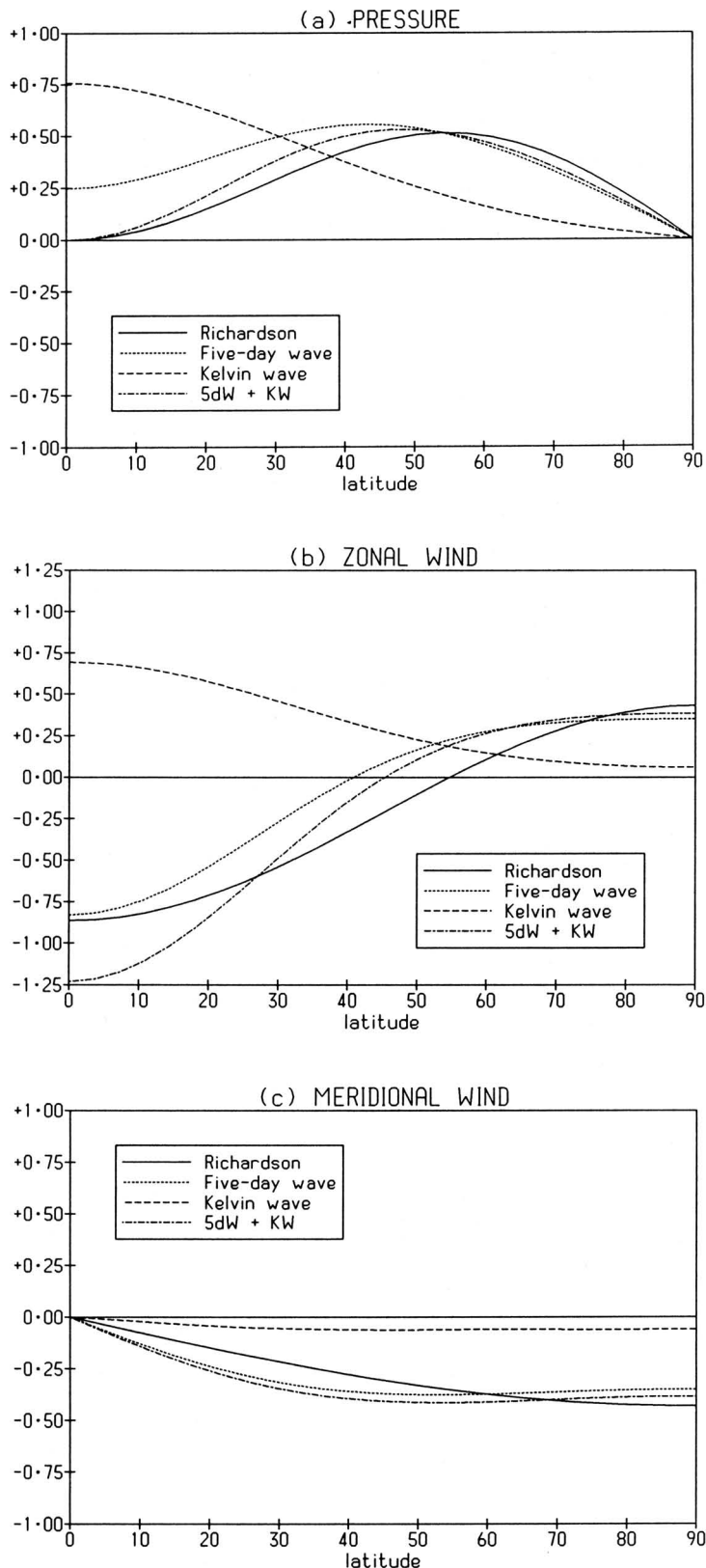


FIG. 7. The meridional structures of (a) pressure at 90°E, (b) zonal wind at 90°E, and (c) meridional wind at 180°E for Richardson's initial pressure and wind perturbations (solid lines), the five-day wave (dotted), the Kelvin wave (dashed), and a linear combination of these two eigenmodes (dot-dash line).

posed on the dominant long-period variation. Referring again to Table 1, the first westward gravity wave has a period of 13.5 h, in good agreement with what is found here. Thus, the temporal variations shown in Fig. 8 can be accounted for by the primary component in each of the three categories: rotational, eastward gravity, and westward gravity waves.

## 7. Filtering the noise

The short-period variations visible in the velocity curves in Fig. 8, and due to the gravity-wave components, may be considered as noise. Such noise is generally undesirable and may be removed by modification of the initial data, a process known as initialization. A simple initialization technique that uses a digital filter will be employed. It is so constructed that high-frequency components are eliminated from the forecast, while long-period variations are virtually unchanged. The noise has a period of about 13 h. Normally it is desirable to preserve the Kelvin wave, which, although a gravity wave, has an important dynamical role. This wave has a period of 34 h. To separate it from the noise, a filter with a cutoff at a period of 24 h was chosen.

The design of the low-pass filter and its application to initialization are described in the Appendix. The fields of pressure and wind resulting from this process are plotted in Fig. 9a. By comparing this with Fig. 4a, one sees that the changes induced by the initialization process are relatively small. Similarly, the one-day forecast starting from initialized data, in Fig. 9b, is very similar to the corresponding forecast from the original data, in Fig. 4b. However, the character of the time evolution is changed in an essential way. The dashed curves in Fig. 8 result from the initialized forecast. The high-frequency oscillations in the wind components, which occurred when using the original data, are almost completely absent now; the initialization has eliminated the noise.

Richardson's baroclinic forecast came to grief through his use of uninitialized data. The unrealistic size of his calculated pressure tendency, 145 hPa in 6 h, was entirely due to anomalously large amplitude grav-

TABLE 2. Expansion coefficients of Richardson's data for the lowest six symmetric modes in each of the three categories. The percentage of total energy in each mode is given in brackets (less than 0.005% indicated as 0.00%).

SYMMETRIC MODE NUMBER	EASTWARD GRAVITY WAVE	WESTWARD GRAVITY WAVE	ROSSBY– HAURWITZ WAVE
1	-0.3302 (10.90%)	0.0751 (0.56%)	0.9196 (84.54%)
2	-0.0029 (0.00%)	-0.0075 (0.01%)	0.1984 (3.93%)
3	0.0003 (0.00%)	-0.0009 (0.00%)	0.0105 (0.01%)
4	0.0003 (0.00%)	-0.0008 (0.00%)	-0.0005 (0.00%)
5	0.0004 (0.00%)	-0.0008 (0.00%)	-0.0009 (0.00%)
6	0.0005 (0.00%)	-0.0009 (0.00%)	-0.0010 (0.00%)

ity-wave components in his initial data. He blamed the failure of his forecast on errors in the wind observations leading to spuriously large values of divergence. However, this is not the whole story; even if changes in the wind field had been contrived to eliminate divergence entirely, high-frequency oscillations would still have ensued.

Richardson did propose several ways to smooth the initial data (LFR, chap. 10). In particular, time-averaging of the data was considered. This is the essence of the digital filtering technique: in the absence of time-series of data, the model equations are used to generate such series, which may then be combined with weights designed to effect the desired smoothing.

Such an option was hardly practicable for Richardson. For effective filtering, the time series must span a period comparable to the desired cutoff. Had he continued his forecast with his chosen time step (3 hours) and his explicit time-stepping scheme, computational instability would have spoiled it. But a time step short enough to guarantee stability would entail unmanageable computation to cover the required span. The only possibility would have been to use an implicit scheme. Richardson sketched in outline such a scheme (LFR, p. 151) but surmised that it was "probably unworkable" on account of the complexity of the simultaneous system of quadratic equations that would arise. Nowadays the implicit method is applied only to the linear gravity-wave terms. The use of a semi-Lagrangian formulation of the advection results in an unconditionally stable scheme allowing large time steps and making the time-filtering initialization scheme feasible.

## 8. Discussion

The introductory example in Richardson's book has been reexamined in the light of advances made since his work was published. His barotropic forecast has been repeated and extended using a global linear shallow-water model. To avoid computational instability that would occur with Richardson's time-stepping scheme, an implicit integration method was employed, yielding a stable forecast with the time step of 3/4 h used by Richardson.

A spectral analysis of Richardson's idealized initial data into the normal modes of the shallow-water equations shows the remarkable preponderance of a single component, the five-day wave. This eigenmode is the symmetric rotational wavenumber-one solution of largest meridional scale. It has been clearly detected in series of atmospheric data. The five-day wave contains almost 85% of the energy of Richardson's fields.

Richardson was unaware of the existence of the five-day wave and other such free waves in the atmosphere. Although these solutions had been studied much earlier by Margules and Hough, an understanding of their geophysical significance became apparent only with the work of Rossby (1939). Richardson regarded the westward movement of his pressure pattern to be in conflict with the generally eastward progression of synoptic systems in middle latitudes, and concluded that "use of the geostrophic hypothesis was found to lead to pressure changes having an unnatural sign" (LFR, p. 146). He seems also to have neglected the dominant influence of the westerlies in the upper troposphere. Although the jet stream was

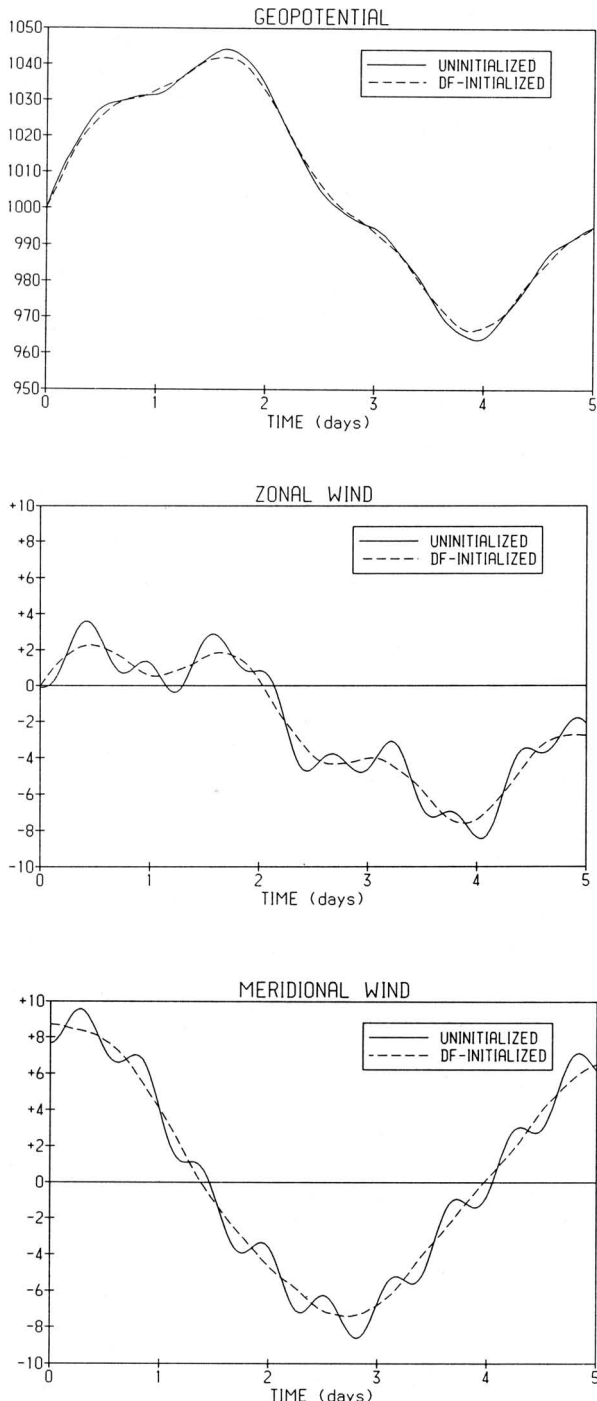


FIG. 8. The time evolution of (a) pressure, (b) zonal wind, and (c) meridional wind at the chosen grid point for the forecast starting from Richardson's data. Solid curves are for the uninitialized data, while dashed curves are for the data initialized by the digital filter.

yet to be discovered, the existence of westerly shear follows from simple balance considerations. Omission of the effect of any background flow in his initial fields could easily have accounted for the disagreement between his barotropic forecast and the observed eastward movement of midlatitude systems.

The baroclinic forecast that forms the centerpiece of Richardson's book was spoiled by high-frequency gravity-wave components in the initial data. These gave rise to spuriously large values of the pressure tendency. Richardson recognized that the divergence field calculated from his data was unrealistic, and he blamed this for the failure of the forecast. However, even if the wind fields were modified to remove divergence completely, high-frequency gravity waves would still be present and cause spurious oscillations. It took many years before this problem was satisfactorily resolved, and meteorological noise could be removed by a modification of the analyzed fields in a process called initialization.

The normal mode analysis of the fields used for the barotropic forecast indicated the presence of a westward-traveling gravity wave with a period of about 13.5 h. This component could be clearly seen in the time traces of the forecast fields. A simple initialization technique, using a digital filter, was applied to the initial fields, and was successful in removing this oscillation without significantly affecting the evolution of the longer-period components. Although the barotropic model is linear, this initialization technique may also be used with a fully nonlinear model.

*Acknowledgments.* I am grateful to my colleague, Dr. Aidan McDonald, for providing the numerical model used in this study. I should also like to express my indebtedness to James P. Koerner, whose extensive comments and suggestions helped me to improve this paper.

## Appendix: Initialization Using a Digital Filter

The height and wind fields defined by Richardson were initialized by application of a digital filter. Some details of the construction of this filter and its application are given below.

Consider a function of time,  $f(t)$ , with low- and high-frequency components. To filter out the high frequencies, we may proceed as follows: 1) Calculate the Fourier transform  $F(\omega)$ ; 2) set the coefficients of the high frequencies to zero; and 3) calculate the inverse transform.

Step 2 may be performed by multiplying  $F(\omega)$  by an appropriate weighting function  $H(\omega)$ . Typically,  $H(\omega)$  is a step function, equal to 1 for  $|\omega| < \omega_c$  and 0 for  $|\omega| > \omega_c$ , with  $\omega_c$  the cutoff frequency. Multiplication of  $F(\omega)$  by  $H(\omega)$  is equivalent to convolution of the corresponding functions in the time domain. Thus, to filter  $f(t)$  we calculate

$$f^*(t) = f * h(t) = \int_{-\infty}^{+\infty} f(\tau)h(t - \tau) d\tau, \quad (A1)$$

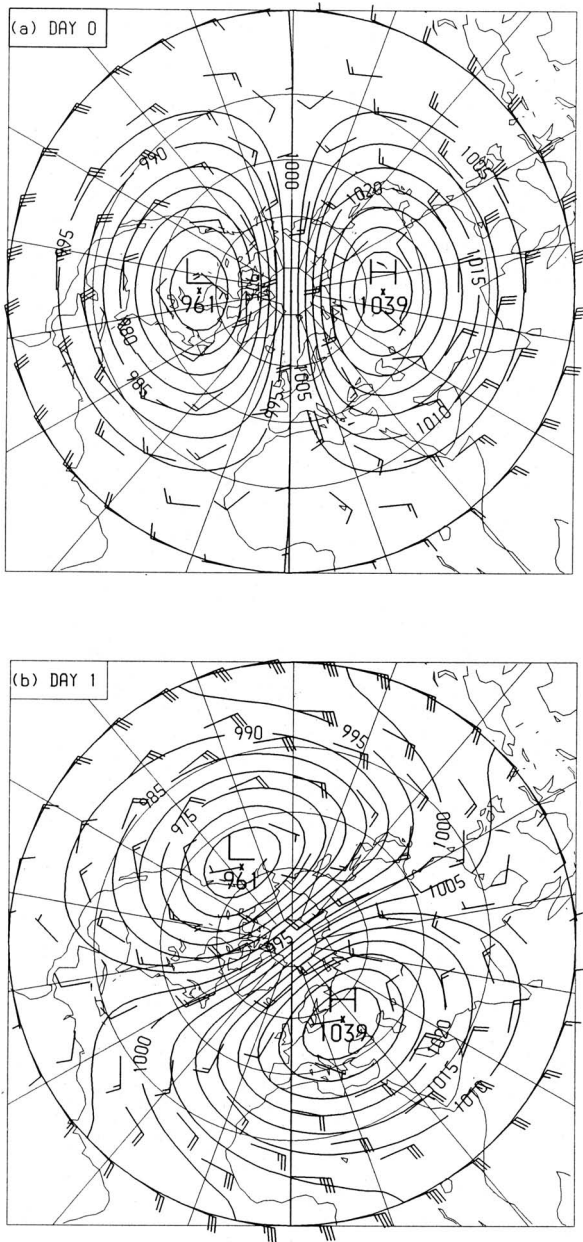


FIG. 9. (a) Pressure and wind fields initialized using the digital filter. (b) One-day forecast resulting from the initialized data.

where  $h(t) = \sin(\omega_c t)/\pi t$  is the inverse Fourier transform of  $H(\omega)$ . To evaluate this integral approximately at  $t = 0$ , we calculate  $f(\tau)$  at a finite set of times  $\{-N\Delta t, \dots, -\Delta t, 0, \Delta t, \dots, N\Delta t\}$  and compute the sum

$$f(0) \doteq \sum_{n=-N}^N f_n h_{-n}, \quad (\text{A2})$$

where  $f_n = f(n\Delta t)$  and  $h_n = \sin(n\omega_c \Delta t)/n\pi$ . As is well known, truncation of a Fourier series may result in Gibbs oscillations. These may be greatly reduced by means of an appropriate window. The response is improved if  $h_n$  is modified by the Lanczos window  $w_n$

$= \sin[n\pi/(N+1)]/[n\pi/(N+1)]$ . For more details, see, for example, Hamming (1989).

The method outlined above was used to calculate filtered fields of height and wind at an initial time. The coefficients of the filter (A2), with a Lanczos window, for parameter values  $\Delta t = 3$  h,  $N = 4$ , and cutoff period  $\tau_c = 2\pi/\omega_c = 24$  h, normalized to have sum unity, are as follows:

$$\begin{aligned} h_0 &= 0.2531 & h_{\pm 1} &= 0.2132 & h_{\pm 2} &= 0.1219 \\ h_{\pm 3} &= 0.0383 & h_{\pm 4} &= 0.0. \end{aligned}$$

The forecast model was used to make three steps forward and three backward, giving heights and winds at seven times centered on  $t = 0$ . Filtered fields were calculated using (A2) with the coefficients given above, for each field at each point. The initialized pressure and wind fields are shown in Fig. 9a, and, by comparison with the original data in Fig. 4a, the changes induced by the initialization are seen to be small.

Although the equations used in this application are linear, the digital filtering technique can be used in precisely the same manner in the case of a nonlinear model. Its advantages are its economy and its great simplicity.

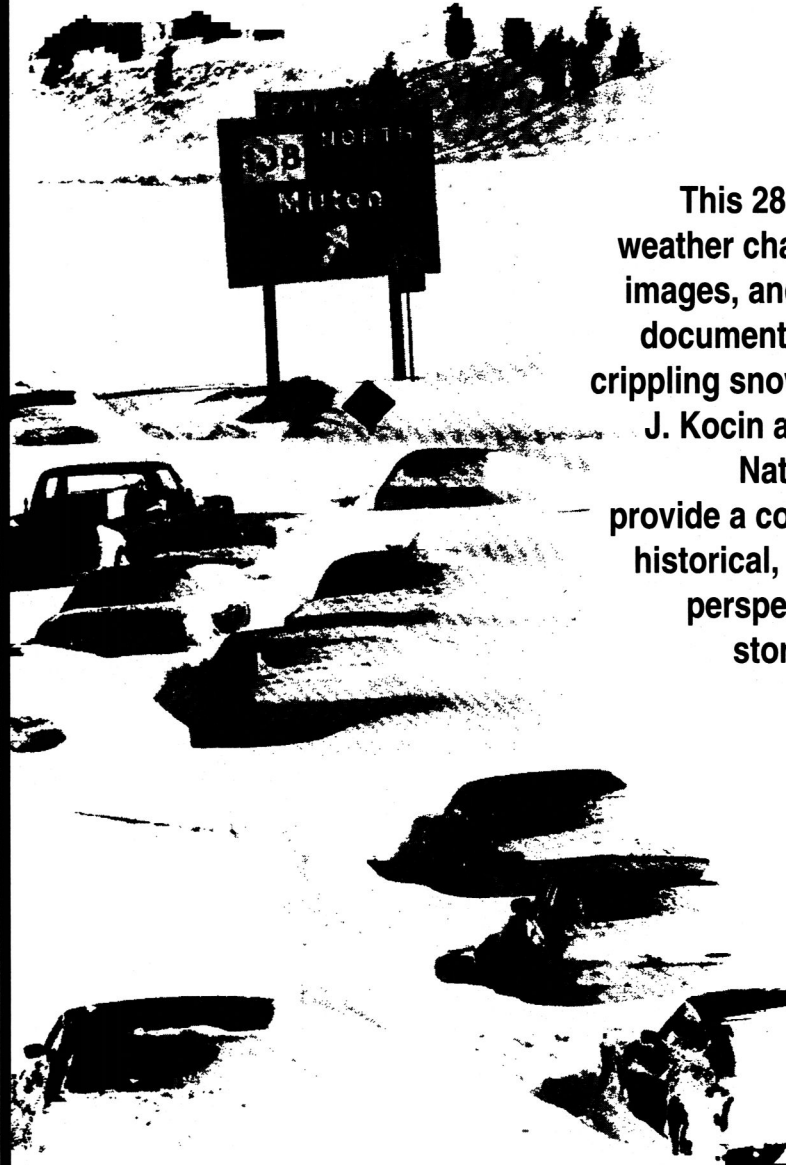
## References

- Debenham, F., 1929: Antarctic regions. *Encyclopaedia Britannica*, XIV Edition. Vol. 2, 14–20.
- Hamming, R.W., 1989: *Digital Filters*. Prentice-Hall, 284 pp.
- Haurwitz, B., 1940: The motion of atmospheric disturbances on the spherical earth. *J. Mar. Res.*, 3, 254–267.
- Kasahara, A., 1976: Normal modes of ultralong waves in the atmosphere. *Mon. Wea. Rev.*, 104, 669–690.
- Longuet-Higgins, M.S., 1968: The eigenfunctions of Laplace's tidal equations over a sphere. *Phil. Trans. Roy. Soc. London*, A262, 511–607.
- Madden, R.A., 1979: Observations of large-scale traveling Rossby waves. *Rev. Geophys. Space Phys.*, 17, 1935–1949.
- McDonald, A., 1986: A semi-Lagrangian and semi-implicit two time-level integration scheme. *Mon. Wea. Rev.*, 114, 824–830.
- , and J.R. Bates, 1989: Semi-Lagrangian integration of a gridpoint shallow-water model on the sphere. *Mon. Wea. Rev.*, 117, 130–137.
- Platzman, G.W., 1967: A retrospective view of Richardson's book on weather prediction. *Bull. Amer. Meteor. Soc.*, 48, 514–550.
- Reid, C., 1976: *Courant in Gottingen and New York*. Springer-Verlag, 256 pp.
- Richardson, L.F., 1922: *Weather Prediction by Numerical Process*. Cambridge Univ. Press, 236 pp. Reprinted by Dover Publications, New York, 1965.
- Rossby, C.G., 1939: Relations between variations in the intensity of the zonal circulation of the atmospheric and the displacements of the semipermanent centers of action. *J. Mar. Res.*, 2, 38–55.
- Sweet, R.A., 1977: A cyclic reduction algorithm for solving block tridiagonal systems of arbitrary dimension. *SIAM J. Numer. Anal.*, 14, 706–720.

# **SNOWSTORMS ALONG THE NORTHEASTERN COAST OF THE UNITED STATES:**

## **1955 TO 1985**

*By Paul J. Kocin and  
Louis W. Uccellini*



This 280-pp. volume, complete with weather charts, color schematics, radar images, and eye-opening photographs, documents 20 of the Northeast's most crippling snowstorms over 30 years. Paul J. Kocin and Louis W. Uccellini, of the National Meteorological Center, provide a comprehensive overview from historical, climatological, and dynamic perspectives to address how these storms develop and forecasters can predict their arrival.

**AMERICAN  
METEOROLOGICAL  
SOCIETY**

©1990, AMS, 280 pp., hardbound. \$32.50/members, \$40/nonmembers includes shipping and handling. Please send prepaid orders to American Meteorological Society, 45 Beacon Street, Boston, MA 02108-3693